Journal of Crystal Growth 413 (2015) 61–66

Contents lists available at ScienceDirect

Journal of Crystal Growth

journal homepage: www.elsevier.com/locate/jcrysgro

X-ray diffraction imaging of ZnTe crystals grown by the multi-tube physical vapour transport technique

J.T. Mullins [a], F. Dierre [a], B.K. Tanner [a,b,*]

[a] Kromek Group plc, Thomas Wright Way, NETPark, Sedgefield, County Durham, TS21 3FD, UK
[b] Department of Physics Durham University, South Road, Durham, DH1 3LE, UK

ARTICLE INFO

Article history:
Received 29 September 2014
Received in revised form
1 December 2014
Accepted 7 December 2014
Communicated by: M. Tischler
Available online 16 December 2014

Keywords:
X-ray topography
High resolution X-ray diffraction
Growth from vapour
Tellurides
Scintillator materials
Semiconducting II-VI materials

ABSTRACT

X-ray diffraction imaging (topography) has been used in monochromatic beam mode to demonstrate that 100 mm diameter ZnTe crystals, several millimetres thick, and grown by the multi-tube physical vapour transport technique on (001) and (211B) GaAs substrates, have very high crystal perfection. Images taken in the Bragg geometry from planes containing the growth direction show evidence of cellular dislocation structure and give strong contrast from the whole, several mm^2, sample area. Rocking curves taken from small areas show only moderate broadening from that expected from a perfect crystal, indicating dislocation density of typically $3.5 \times 10^6\ cm^{-2}$ close to the seed and $3.3 \times 10^5\ cm^{-2}$ at the top of the grown crystal. At the top surface, planes parallel to the seed show biaxial concavity, a feature attributed to the ZnTe boule bowing under tensile strain generated at the substrate-crystal interface due to the mismatch in thermal expansion coefficients of GaAs and ZnTe. Crystals grown on (211B) substrates are of {331} orientation, showing no evidence of twin boundaries, suggesting that {331} growth is initiated at, or very close to, nucleation.

1. Introduction

When doped with oxygen [1], ZnTe shows significant promise as a high-resolution scintillator detector of X-rays and gamma rays due to its high average atomic number, high efficiency, fast decay, low afterglow and excellent spectral match of the oxygen-related luminescence to silicon based detectors. Further, unlike alkali halides, such as sodium iodide, ZnTe is not hydroscopic. However, poor transparency of polycrystalline material limits usable films to less than 1 mm in thickness, and hence to the detection of relatively low energy X-radiation [2,3], making the material uncompetitive for medical imaging.

This interest in ZnTe as a high efficiency scintillator has stimulated recent activity to grow large diameter, optically transparent, high perfection single crystals. In two recent reports, Yan *et al.* [4,5] describe 30 mm diameter ZnTe crystals grown from Te solution by the vertical Bridgman method with an accelerated crucible rotation technique. These, however, contain Te inclusions as well as grain boundaries and twins. Shkir *et al.* [6] had previously reported 19 mm diameter crystals grown by the vertical Bridgman method, showing high resolution X-ray diffraction (HRXRD) rocking curves of 58 arc sec full width at half height maximum (FWHM) from parts of the samples. Melt growth techniques for ZnTe are not new. Indeed, ZnTe crystals grown on sapphire substrates were produced by the vertical gradient freeze method [7] as early as 1998. These 44 mm diameter boules were 70% single crystal across the wafer but contained misoriented grains at the edges. From selected areas, 20 arc sec HRXRD rocking curves were obtained. Crystals up to 80 mm diameter were grown during this period [8–10]. 15 mm diameter boules containing some misoriented grains, but which were 80% single crystal, were also reported by Uen *et al.* [11] using a temperature gradient solution growth method.

Vapour growth of large diameter ZnTe has a similar history, with 40–50 mm diameter crystals reported in 2000 using a seeded vapour growth from a polycrystalline seed [12]. HRXRD rocking curve widths 18–22″ were claimed but not shown in the paper. However, more recent vapour transport attempts have been less impressive [13,14]. In 1999, we described the characteristics of CdTe crystals grown by a multi-tube physical vapour transport (MTPVT) technique [15] and have subsequently reported the growth of large diameter and volume CdTe [16] and CdZnTe [17] crystals using GaAs seeds. In this article, we present an X-ray diffraction imaging study of samples cut from 100 mm diameter ZnTe crystals grown by this method and show that they have very high crystal lattice perfection.

2. Experimental methods

Crystals of ZnTe (Fig. 1(a)), 100 mm diameter and up to 10 mm thickness, with and without oxygen doping, have been grown on

* Corresponding author at: Department of Physics, Durham University, Durham DH1 3LE, U.K. Tel.: +44 191 3343677.
E-mail address: b.k.tanner@dur.ac.uk (B.K. Tanner).

http://dx.doi.org/10.1016/j.jcrysgro.2014.12.007
0022-0248/

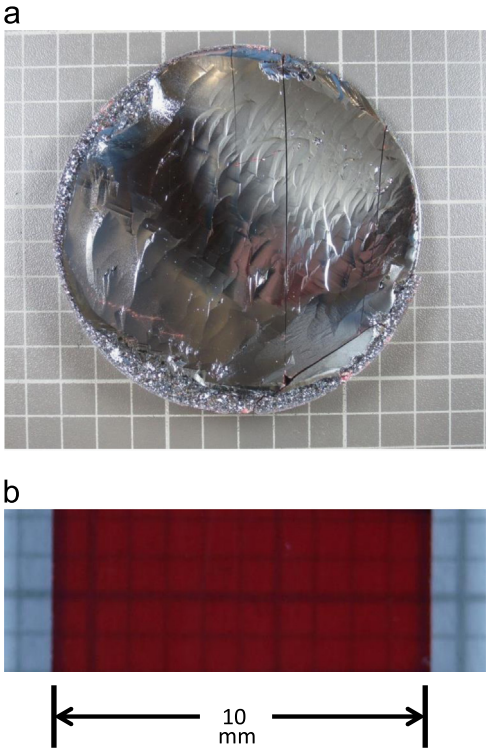

Fig. 1. (a) Photograph of a 100 mm diameter, 7 mm thick ZnTe crystal grown by MTPVT, on its GaAs (001) seed. (b) 1.5 mm thickness slice of an undoped crystal, illustrating its optical transparency.

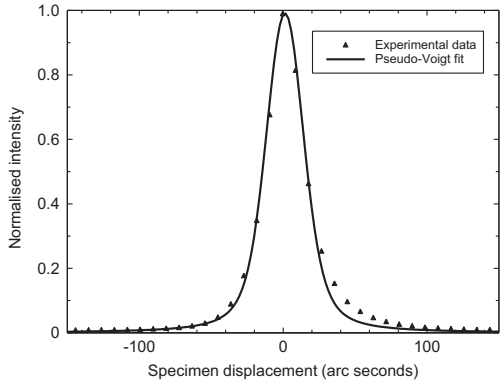

Fig. 2. Rocking curve taken from the (110) face of a cube-oriented ZnTe crystal.

(001) and (211B) oriented GaAs seed wafers located within a quartz growth envelope containing the source material [18]. The undoped crystals were optically transparent (Fig. 1(b)). Details of the growth system can be found in the paper by Mullins *et al.* [19], its key feature being that the temperature of source and seed are thermally decoupled by use of independent vertical furnaces which are parallel, separated horizontally and interconnected by a horizontal, heated, transport tube to avoid any line of sight, and thus radiative thermal coupling, between source and seed. The growth envelope is constructed from quartz and together with the surrounding heating elements is contained within an evacuated and cooled stainless steel chamber. Flow restrictors incorporated into the horizontal transport tube effectively de-couple the mass transport from the source – sink temperature difference making the growth process highly controllable. Oxygen doping was achieved through use of nitrous oxide gas, fed into the evacuated quartz growth envelope via two flow-restricting orifices. The pressure in the space between the orifices can be set using an auxiliary pump and throttle valves allowing a small, controllable gas flow into the growth region

X-ray diffraction imaging (topography) [20] in the Bragg (reflection) geometry was undertaken using the Huber diffractometer at beamline B16 of the Diamond Light Source at Didcot, UK. All images shown in this paper were taken using an energy of 10 keV, the beam being monochromated by a pair of independently tuned 111 Si reflections. The imaging detector was a Photonic Science SCMOS camera with a pixel pitch of 3.25 μm. Topographs are reproduced as positives (with enhanced intensity darker) looking towards the X-ray source. The incidence plane is always vertical. Rocking curves were obtained from the sum of the signal from all of the camera pixels in a frame. Short integration times were used for rocking curve measurement in order to avoid saturation of individual pixels. (We note that non-linearity due to saturation tends to broaden, rather than sharpen, the rocking curve FWHM.) Samples were cut with side faces parallel and perpendicular to the {110} orientation flat on the GaAs seeds. They were lapped, then polished using a 3 μm diamond suspension on fabric polishing pads and finally etched for two minutes in a solution of 2% bromine in methanol at 21 °C to remove the residual strain associated with the polishing process.

3. Results

The 220 reflection rocking curve taken with an extended beam, covering the whole 10 mm × 3 mm area of the (110) face of a cube-oriented ZnTe crystal grown on a (001) GaAs seed is shown in Fig. 2. The first noteworthy observation is that not only is the sample entirely single crystal and contains no sub-grains, but that the rocking curve width over this large area is 32 ± 1arc sec FWHM. As we show below, the rocking curve FWHM can depend very strongly on the beam size and this uniformity, found on all crystal faces containing the growth axis that we have examined, indicates the establishment of extremely stable growth conditions. The second feature of rocking curves from faces containing the growth axis, and found in both (001) and (211B) seeded crystals, is an asymmetric tail on the high angle side. It is made obvious from the (symmetric) pseudo-Voigt fit to the data shown in Fig. 2.

Fig. 3 shows four double axis X-ray topographs of the crystal face from which the rocking curve of Fig. 2 was recorded. Fig. 3(a) is taken from the peak of the rocking curve. It is typical of all the samples examined. There are high intensity regions right across the sample face indicating that the curvature of the lattice planes containing the growth direction is very small. Little bowing of the crystal occurs as it grows. The dislocation density appears to be too high to resolve individual dislocations with any confidence but the high diffracted intensity regions cluster into cellular features suggesting that some polygonisation of the underlying dislocation structure has occurred. There are larger regions which appear light. Several of these appear dark in the topograph taken at displacement -18 arc sec. with respect to the rocking curve peak (Fig. 3(b)), indicating that the crystal planes are here misoriented negatively by this amount with respect to the majority of the material. Sharp sub-grain boundaries are not, however, observed. Topographs taken from the asymmetric tail of the rocking curve, Fig. 3(c) and (d), show diffracted intensity increasingly confined to the region of the crystal adjacent to the seed (on the right hand side of the image). Increasing angular displacement results in lower intensity but this continues to come from the near-seed region.

The 240 type reflections have the Bragg planes asymmetric with respect to the {110} surfaces such that, with 10 keV X-radiation, the incidence angle is grazing at 8.58° to the surface. Such a reflection has a lower penetration depth and is more sensitive to surface strains. There is, nevertheless, no significant difference in the topographic images of the 240, 220 (and 440) reflections. The $\bar{2}40$ reflection from the $(\bar{1}10)$ face, Fig. 4, does make the cellular nature of the defect structure more prominent. In this reflection